Available online at www.sciencedirect.com

ScienceDirect

Ceramics International 40 (2014) 11–16

CERAMICS INTERNATIONAL

www.elsevier.com/locate/ceramint

Crystallization, structure and fluorescence emission of Nd^{3+}- and Yb^{3+}-doped NCS transparent glass-ceramics

Anxian Lu[a], Xiaolin Hu[a], Yajun Lei[a], Zhiwei Luo[a], Xiuying Li[b,*]

[a]School of Materials Science and Engineering, Central South of University, Changsha 410083, PR China
[b]School of Minerals Processing and Engineering, Central South of University, Changsha 410083, PR China

Received 9 April 2013; received in revised form 15 April 2013; accepted 15 April 2013
Available online 24 April 2013

Abstract

Nd^{3+}- and Yb^{3+}-doped glasses and highly crystalline transparent glass-ceramics in the Na_2O–CaO–SiO_2 (NCS) system have been successfully prepared. Compared with Nd^{3+}-doped NCS glass, the Yb^{3+}-doped NCS glass has a stronger crystallization trend. The Nd^{3+}- and Yb^{3+}-doped NCS glass-ceramics contain about 84.35 ± 5 vol% of $Na_6Ca_3Si_6O_{18}$ and 87.03 ± 5 vol% of $Na_4Ca_4Si_6O_{18}$, respectively. The two crystal phases have the same basic structural units composed of 6-membered rings formed by 6 [SiO_4] groups but the phase in the Yb^{3+}-doped NCS glass-ceramics has a composition ratio more similar to its parent glass. The transmittance of the Yb^{3+}-doped NCS glass-ceramics is higher than that of Nd^{3+}-doped sample. Strong fluorescence emissions have been observed for the Nd^{3+}-and Yb^{3+}-doped NCS glass-ceramics, which indicates the potential of rare earth ions-doped highly crystalline transparent glass-ceramics for use as laser medium materials.

Keywords: D. Glass; Highly crystalline; Transparent glass-ceramics; Transmittance; Fluorescence emission

1. Introduction

Transparent crystals and transparent ceramics including Gd_2SiO_5(GSO) [1–4], $YAlO_3$(YAP) [5–7], $Y_3Al_5O_{12}$(YAG) [8–11], $Gd_3Ga_5O_{12}$(GGG) [12–14] and Al_2O_3–Si_3N_4 [15,16] have a wide range of applications as infrared generator, solid-state lasers, infrared dome, nuclear imaging system, high energy particle detectors and CT scanners. However, some technical obstacles in their preparation are difficult to overcome [17] because of their limited dimensions, high requests to equipment and raw materials. Specially, it is very difficult to adjust the properties of transparent crystals and ceramics by means of altering components due to their high selectivity to chemical compositions. Compared with crystals and ceramics, larger size glass-ceramics can be produced by glass-forming and subsequent heat treatment process (nucleation and crystallization). Meanwhile, the basic physical and chemical properties of a material depends mainly on its matrix and structure, while the functional characteristics, such as laser and scintillating performances, depend on the functional components added into their matrix. Transparent glass-ceramic is a multi-composition system, in which the chemical compositions of glass matrix and functional components can be varied in a wide range. Usually, small amount of impurities does not affect the structure and performance of main crystal phase in glass-ceramics. Therefore, it is possible that the high crystalline transparent glass-ceramics substitute for transparent crystals and ceramics.

In principle, the highly crystalline transparent glass-ceramics with special functions can be prepared by adding rare earth ions Ce^{3+}, Pr^{3+}, Nd^{3+}, Sm^{3+}, Tb^{3+}, Er^{3+}, and Yb^{3+} into glass matrix. The transparent glass-ceramics containing above rare earth ions may substitute for scintillating crystals or transparent ceramics including rare earth ions doped GSO, YAP, YAG, GGG, Al_2O_3–Si_3N_4, spinel ($MgAl_2O_4$), and $(Y,Gd)_2O_3$ (YGO). Unfortunately, it is very difficult to prepare the transparent glass-ceramics based on above various compositions. In future development of highly crystalline transparent glass-ceramics

*Corresponding author. Tel.: +86 731 88830351; fax: +86 731 88877057.
E-mail addresses: axlu@mail.csu.edu.cn (A. Lu), x.y.lio731csu@163.com (X. Li).

0272-8842/$ - see front matter © 2013 Published by Elsevier Ltd and Techna Group S.r.l.
http://dx.doi.org/10.1016/j.ceramint.2013.04.049

containing above the crystal phases, there are two important problems to consider. One is how to prepare basic glasses and obtain highly crystalline transparent glass-ceramics. The other is the effects of introducing rare earth or transition metal ions into the basic glasses on glass formation, crystallization, especially optical and spectroscopic properties. Obviously, there are many scientific and technological problems existing in the research for these glass-ceramics. Optimistically, a few of highly crystalline transparent glass-ceramics have been prepared successfully, such as Na_2O–CaO–SiO_2 (NCS) [18–21], Nd^{3+}-doped NCS [22–24] and Yb^{3+}-doped NCS [25] glass-ceramics. If the preparation techniques of rare earth ions doped transparent NCS glass-ceramics can be popularized to other glass systems, it is possible to prepare the highly crystalline transparent glass-ceramics with the functional properties similar to the crystal or transparent ceramics based on GSO, YAP, YAG, GGG, Al_2O_3–Si_3N_4, $MgAl_2O_4$, and YGO. Clearly, it is meaningful to study systematically NCS glass-ceramics.

In all published papers, only one paper [25] deals with the preparation and microstructure of Yb^{3+}-doped NCS glass-ceramics. No article describes the differences in crystallization, structure and fluorescence emission between Nd^{3+}- and Yb^{3+}-doped NCS transparent glass-ceramics as well as the crystallization mechanism, structure of phase, absorption spectrum, emission spectrum of Yb^{3+}-doped NCS glass-ceramics. In present study, $17Na_2O$–$30CaO$–$53SiO_2$ (wt%) was chosen as the basic compositions of NCS glass-ceramics doped rare earth ions according to the optimized results obtained by the authors [23,25]. The main aim is to investigate the differences in crystallization, phase, microstructure, transmission in visible region, absorption and emission spectra between Nd^{3+}- and Yb^{3+}-doped highly crystalline transparent glass-ceramics based on $17Na_2O$–$30CaO$–$53SiO_2$ (wt%).

2. Experimental procedure

2.1. Starting materials

The starting materials were analytically pure $CaCO_3$(99.9 wt %), Na_2CO_3(99.8 wt%), SiO_2(99.9 wt%), Nd_2O_3(99.99 wt%) and Yb_2O_3(99.99 wt%) powders, in which CaO and Na_2O were introduced by high temperature decomposition of $CaCO_3$ and Na_2CO_3 during glass melting, respectively. The Nd^{3+} and Yb^{3+} ions were introduced by adding 2 wt% Nd_2O_3 and 2 wt% Yb_2O_3 into the glasses.

2.2. Preparation of the glasses

The batch mixed thoroughly after weighing precisely (the precision is 0.01 g) was put in alumina crucible and melted at 1500 °C for 2 h in electric furnace. After melting and clarifying, the glass melt was poured onto preheated iron plate, then put into muffle furnace to anneal at 580 °C for 3 h for eliminating the residual thermal stress in the glass. After cooling to room temperature, the two precursor glasses were prepared.

2.3. DSC measurement

A differential scanning calorimeter (short for DSC, NETZSCH 449PC, Germany) was used to measure the transition temperature T_g, initial crystallization temperature T_{ic}, crystallization peak temperature T_p and thermo-stabilizing parameter $\Delta T(\Delta T=T_{ic}-T_g)$ of the parent glasses in order to provide the reference about the nucleating and crystallization temperature of the parent glasses.

2.4. Preparation of the glass-ceramics

Based on the results of DSC measurement, T_g, T_{ic}, T_p and ΔT of the Nd^{3+}-doped NCS glass is 626 °C, 771.2 °C, 805.1 °C and 145.2 °C, respectively. The glass sample was heated at 800 °C for 1.0 h after nucleating at 630 °C (slightly higher than T_g) for 10 h for preparing glass-ceramic. The crystallization temperature was higher than initial crystallization temperature 771.2 °C but near the crystallization peak temperature 805.1 °C on the DSC. Compared to the Nd^{3+}-doped NCS glass, the Yb^{3+}-doped NCS glass has lower T_g(614.5 °C), T_{ic}(710 °C), T_p(731 °C) and ΔT(95.5 °C). According to our experiments, when the Yb^{3+}-doped NCS glass was treated from 595 °C to 655 °C for nucleating at a constant crystallization temperature, their crystalline and transmittance did not appear obvious change. Therefore, the glass sample was heated at 730 °C (near T_p) for 1.0 h after treating at 595 °C (slightly lower than T_g) for 5 h for preparing transparent glass-ceramic. The Nd^{3+}- and Yb^{3+}-doped glasses and glass-ceramics are shown in Fig. 1.

The samples with different sizes by cutting the glass-ceramics were optically polished in order to meet different measurements requirement. For the optical measurements, the sample dimensions are 15 mm × 15 mm × 3 mm.

2.5. Characterization

The XRD patterns of the glass-ceramic powder samples were recorded by a Rigaku D/max2500 PC X-ray (CuKα,

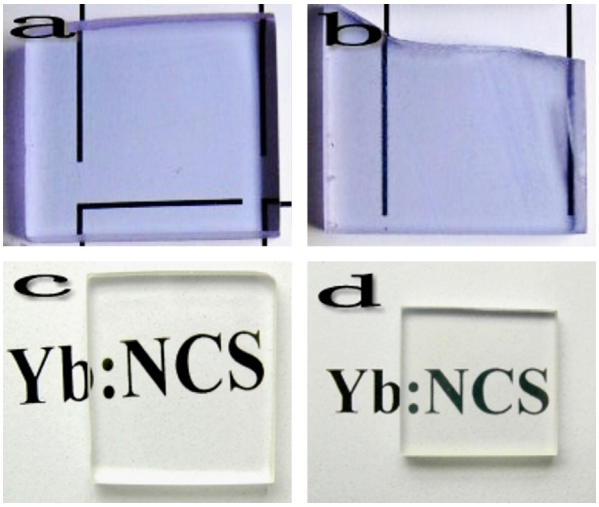

Fig. 1. The samples for Nd^{3+}- and Yb^{3+}-doped glasses and glass-ceramics in NCS system: (a) Nd^{3+}-doped glass, (b) Nd^{3+}-doped glass-ceramic, (c) Yb^{3+}-doped glass, and (d) Yb^{3+}-doped glass-ceramic.

scanning rate 8°/min, and scanning range 10–80°). The phases in the glass-ceramics were determined by using JCPDF cards. MDI Jade 5.0 software (Materials Data Inc, Liverpool, CA) was used to analyze the XRD patterns. The crystallinity of glass-ceramics was calculated as the ratio of the intensity under the crystalline peaks above the background to the total intensity [23,26]. The calculated error is ±5 vol%. The micro-structures of glass-ceramics were observed by the scanning electron microscopy named as Quanta 200. The transmissions in visible region of the glass-ceramics were recorded with a HITACHI U-3310 UV spectrophotometer from 400 nm to 1100 nm. The absorption spectra of the glass-ceramics were obtained at room temperature with a UV–VIS–NIR spectrophotometer (Lambda-900, Perkin-Elmer Corporation). The emission spectra of the glass-ceramics were acquired by using a spectrophotometer (Edinburgh Instruments Ltd., Flsp920) with an 808 nm laser diode (LD) acted as the excitation source.

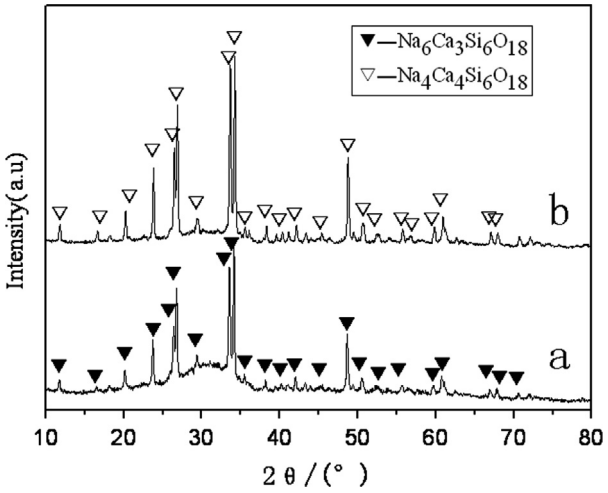

Fig. 2. The XRD patterns of the Nd^{3+}-doped and Yb^{3+}-doped NCS glass-ceramics: (a) Nd^{3+}-doped glass-ceramic and (b) Yb^{3+}-doped glass-ceramic.

3. Results and discussion

3.1. Crystallization trend

Generally, the higher ΔT of a glass is, the better its thermostability is, which indicates that the crystallization of the glass is more difficult. The Y^{3+}-doped NCS glass has lower ΔT and shows an easier crystallization compared to the Nd^{3+}-doped NCS glass. This can be explained from different electronic structures of Nd^{3+} and Yb^{3+} ions. It is well known that Nd and Yb belongs to the lanthanide system, their atomic number and outer electron structure are 60, $4f^46s^2$ and 70, $4f^{14}6s^2$, respectively. In glass, the electronic structure of their outer layer are converted into $4f^3$ (for Nd^{3+} ions) and $4f^{13}$ (for Yb^{3+} ions). Due to lanthanide contraction effects, the ionic radius decrease with the increasing of atomic number from lanthanum to lutetium. Yb^{3+} ion has smaller ionic radius and a stronger ability to attract O^{2-} ions in the glass. As a result, Yb^{3+}-doped NCS glass shows an easier crystallization trend than Nd^{3+}-doped NCS glass.

3.2. Crystal phase and crystalline

Fig. 2(a) and (b) shows the XRD pattern of Nd^{3+}-doped NCS glass-ceramic (sample b) and Yb^{3+}-doped NCS glass-ceramic (sample d), respectively. The sharp diffraction peaks can be observed on the XRD patterns of the two glass-ceramics due to precipitating a large number of micro-crystals from the parent glasses during the heat treatment of the glass. Compared with the pattern of Yb^{3+}-doped NCS glass-ceramic as shown in Fig. 2(b), more obvious scattered feature can be observed from the XRD pattern of Nd^{3+}-doped glass-ceramic as shown in Fig. 2(a). This means that the Nd^{3+}-doped glass-ceramic contains slightly more glass phase and lower crystal phase than Yb^{3+}-doped NCS glass-ceramic.

As shown in Fig. 2, both Nd^{3+}-and Yb^{3+}-doped NCS glass-ceramics only contain single crystal phase. For the $17Na_2O$–$30CaO$–$53SiO_2$ glass-ceramic containing 2 wt% of Nd_2O_3 (sample b), the single crystal phase is determined as $Na_6Ca_3Si_6O_{18}$ ($3Na_2O \cdot 3CaO \cdot 6SiO_2$) (PDF No 77-2189), in which the content of Na_2O, CaO and SiO_2 is 26.02, 23.54 and 50.44 wt%, respectively. The calculated crystalline of the glass-ceramic by the Jade 5.0 software is 84.35 ± 5 vol%. For the $17Na_2O$–$30CaO$–$53SiO_2$ glass-ceramic with 2 wt% of Yb_2O_3 (sample d), the crystal phase is determined as $Na_4Ca_4Si_6O_{18}$ ($2Na_2O \cdot 4CaO \cdot 6SiO_2$) (PDF No 78-0364) which contains 17.50% of Na_2O, 31.68% of CaO and 50.91% of SiO_2 in weight percentage. The calculated crystalline of the glass-ceramics is 87.03 ± 5 vol%. The results are consistent with the above X-ray diffraction analysis. Compared to $Na_6Ca_3Si_6O_{18}$ phase, $Na_4Ca_4Si_6O_{18}$ phase has a composition ratio more similar to the $17Na_2O$–$30CaO$–$53SiO_2$ parent glass. It is clear that $Na_6Ca_3Si_6O_{18}$ and $Na_4Ca_4Si_6O_{18}$ have the same basic structural units composed of 6-membered rings formed by 6 [SiO_4] groups (6 [SiO_4] groups constitutes one 6-membered ring).

It is known that pure SiO_2 glass has a complete three-dimensional network structure constituted by [SiO_4] tetrahedral. With the introduction of alkali and alkaline earth metal oxides, its three-dimensional network structure is gradually depolymerized. In the present study, the glass contains lower content of SiO_2 (53 wt%), and higher content of Na_2O (17 wt %) and CaO(30 wt%). Obviously, there are many network discontinuous points (Si–O^-/$^-$O–Si) existing in the glass structure due to interrupted direct connection among 6-membered rings formed by 6 [SiO_4] groups. Na^+, Ca^{2+} and Nd^{3+} ions or Na^+, Ca^{2+} and Yb^{3+} ions situate the discontinuous points and join O^{2-} ions in the glass structure. On the one hand, Yb^{3+} ion has stronger agglomerating effects due to its smaller ionic radius than that of Nd^{3+} ion, which results in an easier crystallization during the heat treatment of the glass. These strong absorption peaks above a few wavelength positions indicate that the prepared glass-ceramics possess expected emission wavelength for use as laser medium materials. Since Na–O bond is weaker than that of Ca–O bond, Nd^{3+} or Yb^{3+} ions in the residual glass will preferentially attract the oxygen ions in Na_2O rather than ones in CaO.

During crystallization, it is easier for $Ca^{2+}$and relevant coordination O^{2-} to participate in the constitution of precipitated phase than Na^{+} and related O^{2-}. At the same time, the ability of Yb^{3+} for attracting O^{2-} ions is stronger than that of Nd^{3+}; Yb^{3+} ions in the residual glass will attract more oxygen ions in Na_2O, which indicates that more Na^{+} ions will be retained in the glass phase for maintaining the electrical neutrality of the system. As a result, the crystal phase in Yb^{3+}-doped NCS glass-ceramic has lower content of Na_2O and higher content of CaO compared to Nd^{3+}-doped NCS glass-ceramic.

3.3. Microstructure

The SEM photos of Nd^{3+}- and Yb^{3+}-doped NCS glass-ceramics are shown in Fig. 3. It can be seen from Fig. 3 that a larger number of crystal grains with μm size distribute evenly in the amorphous medium. From XRD results, the basic structure unit in these grains is 6-membered ring formed by 6 [SiO_4] groups. These rings are linked by the bridge oxygen in the micro-crystal structure, which constitutes three-dimensional network structure of the micro-crystals. The part lattice positions in micro-crystals were occupied by Ca^{2+} and Na^{+} for forming $Na_6Ca_3Si_6O_{18}$ or $Na_4Ca_4Si_6O_{18}$ phase with orderly arrangement. Similar to the crystal structure, the basic structural unit in these glasses is also 6-membered ring formed by 6 [SiO_4] groups. These rings are linked by the bridge oxygen in the glass structure. The disorderly arrangement of the 6-membered rings constitutes three-dimensional network structure of the glass. The intermittent points in the glass network structure are linked by Na^{+}, Ca^{2+} and Nd^{3+} or Na^{+}, $Ca^{2+}$and Yb^{3+} for holding the balance of valent state. The crystal grains are agglutinated by Nd^{3+}- or Yb^{3+}-doped NCS glass phase. Compared with Nd^{3+}-doped NCS glass, despite Yb^{3+}-doped NCS glass undergone lower temperatures of nucleation and crystallization and shorter time of nucleation, its crystal size is obviously larger than that of Nd^{3+}-doped NCS glass-ceramics, which is attributed to the stronger crystallization trend of Yb^{3+}-doped NCS glass. In addition, adopted different corrosion conditions for measuring the SEM also effect the difference of morphologies shown on two photos.

3.4. Color and transmission in visible region

As shown in Figs. 1 and 4, there is an obvious difference in the color between Nd^{3+}- and Yb^{3+} -doped samples. The colorless glass and glass-ceramics have been observed from Yb^{3+}-doped NCS samples because there is no obvious absorptions caused by Yb^{3+} ions in visible region (generally, from 380 nm to 780 nm). Compared with Yb^{3+} ions, Nd^{3+} ions have strong absorptions at about 530 nm, 580 nm, and 750 nm due to the electronic transition from ground state to excited state of Nd^{3+} ions, which results in the color of Nd^{3+} doped NCS glass and glass-ceramic. It is also observed that Nd^{3+}-doped NCS glass and its glass-ceramic or Yb^{3+}-doped NCS glass and its glass-ceramic have similar appearances and approximate transmission in visible region, this means that the electronic structure of Nd^{3+} or Yb^{3+} ions did not obviously change when the glasses were treated into glasses-ceramics.

It can be seen from Fig. 4 that transmittances of the Nd^{3+}-and Yb^{3+}-doped NCS glass-ceramics are higher than 80% from 400 nm to 1100 nm for 3 mm samples. Generally, the requirement is that the size of particles in glass-ceramics is small enough (for example, less than 80 nm) or the difference in the refractive index

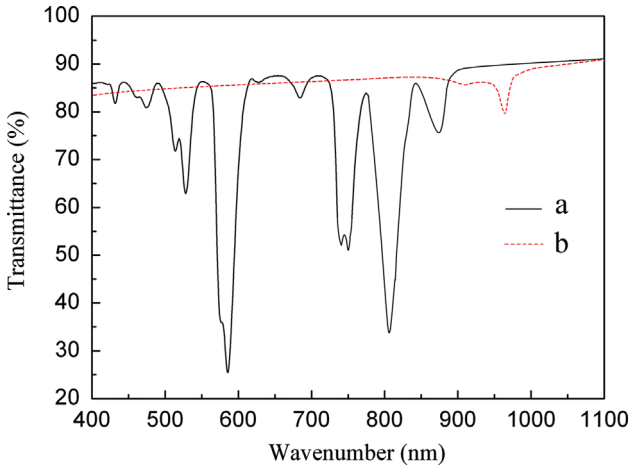

Fig. 4. The transmission spectra of the Nd^{3+}-doped NCS and the Yb^{3+}-doped NCS glass-ceramics: (a) Nd^{3+}-doped glass-ceramic and (b) Yb^{3+}-doped glass-ceramic.

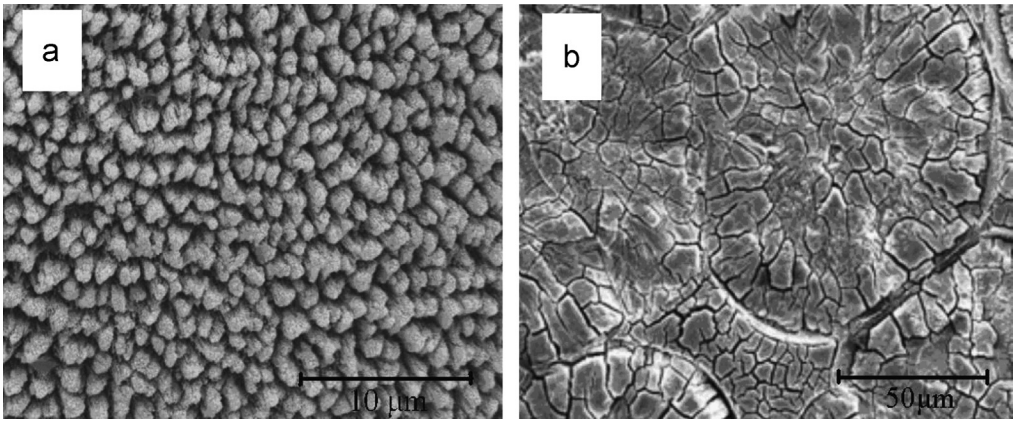

Fig. 3. The SEM photos of the Nd^{3+}-doped NCS and the Yb^{3+}-doped NCS glass-ceramics: (a) Nd^{3+}-doped glass-ceramic and (b) Yb^{3+} -doped glass-ceramics.

in the phases is almost the same in order to prepare the glass-ceramics with high transparency. The size of most particles is larger than 1 μm for the prepared glass-ceramics, their high transmittance is attributed to a minimal difference of refractive index between the crystal and glass because both have similar chemical composition ratio. The absorptions of sample b at about 530 nm, 580 nm, 750 nm, 820 nm and 880 nm were caused by the electron transition from ground state to excited state in Nd^{3+} ions. Similarly, the absorption of sample d at about 970 nm was caused by the electron transition in Yb^{3+} ions. These strong absorption peaks above a few wavelength positions indicate that the prepared glass-ceramics possess expected emission wavelength for use as laser medium materials.

3.5. Absorption and emission spectrum

Fig. 5 shows the absorption and emission spectrum of the Nd^{3+}-doped NCS glass-ceramics(sample b). As shown in Fig. 5(a), ten absorption bands were observed from the spectrum, which correspond to the transitions from ground state $^4I_{9/2}$ to higher energy levels of $4f^3$ electronic configuration of Nd^{3+} ions in the glass-ceramics, including $^4I_{9/2}\rightarrow{}^4F_{3/2}$, $^4F_{5/2}+{}^2H_{9/2}$, $^4F_{7/2}+{}^4S_{3/2}$, $^4F_{9/2}$, $^2H_{11/2}$, $^4G_{5/2}+{}^2G_{7/2}$, $^2K_{13/2}+{}^4G_{7/2}+{}^4G_{9/2}$, $^4G_{11/2}+{}^2G_{9/2}+{}^2D_{3/2}+{}^2K_{15/2}$, $^2P_{1/2}+{}^2D_{5/2}$ and $^4D_{5/2}+{}^4D_{3/2}+{}^2I_{11/2}$[22]. Three stronger absorption bands appear at about 580 nm, 750 nm and 810 nm, which were caused by the transitions from $^4I_{9/2}\rightarrow{}^4G_{5/2}+{}^2G_{7/2}$, $^4I_{9/2}\rightarrow{}^4F_{7/2}+{}^4S_{3/2}$ and $^4I_{9/2}\rightarrow{}^4F_{5/2}+{}^2H_{9/2}$, respectively. It can be seen from Fig. 5(b) that three emission bands of the Nd^{3+}-doped NCS glass-ceramics appear at about 880 nm, 1060 nm and 1320 nm(excited at 809 nm), which are assigned to the transitions from $^4F_{3/2}\rightarrow{}^4I_{9/2}$(~900 nm), $^4F_{3/2}\rightarrow{}^4I_{11/2}$(~1060 nm) and $^4F_{3/2}\rightarrow{}^4I_{13/2}$(~1300 nm), respectively [27].

Generally, the absorption spectra of Yb^{3+}-doped glasses or glass-ceramics can resolve into three bands in the range from 900 nm to 1100 nm since the excited state $^2F_{5/2}$ of Yb^{3+} ions is likely to split into three levels. Fig. 6 shows the absorption and emission of the Yb^{3+}-doped NCS glass-ceramics (sample d). As shown in Fig. 6(a), two obvious absorption peaks and one very weak peak were observed at about 975 nm, 910 nm and 950 nm, respectively. The strongest absorption band (near 975 nm) corresponds to the transitions from ground state $^2F_{7/2}$ to excited state $^2F_{5/2}$. The stronger band (near 910 nm) and the weak band at about 950 nm are attributed to the energy level splitting of excited state $^2F_{5/2}$ of Yb^{3+} ions. From the Fig. 6(b), the emission spectrum of the Yb^{3+}-doped NCS glass-ceramics (excited at 970 nm) exhibits two strong bands at about 975 nm and 1100 nm due to the

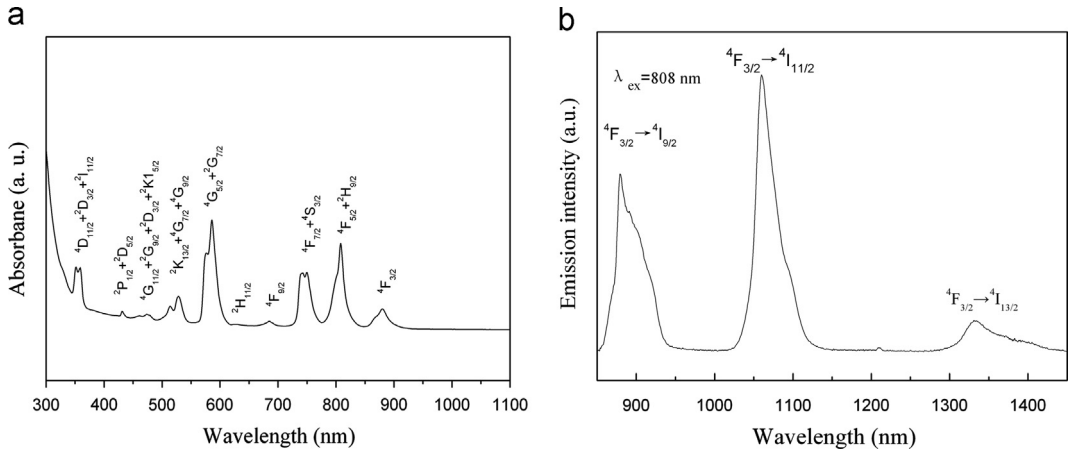

Fig. 5. The absorption and emission spectrum of the Nd^{3+}-doped NCS glass-ceramics: (a) absorption spectrum and (b) emission spectrum.

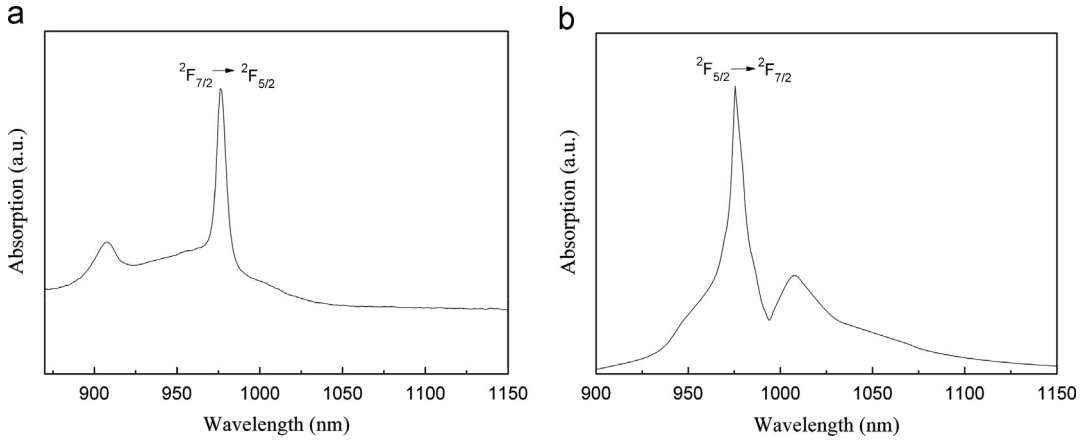

Fig. 6. The absorption and emission spectrum of the Yb^{3+}-doped NCS glass-ceramics: (a) absorption spectrum and (b) emission spectrum.

electronic transitions from the split energy levels of excited state $^2F_{5/2}$ to ground state $^2F_{7/2}$.

4. Conclusions

Nd^{3+}- and Yb^{3+}-doped glasses and highly crystalline transparent glass-ceramics in the NCS system have been successfully prepared by conventional melt quenching technology and subsequent crystallization process. Compared with Nd^{3+}-doped NCS glass, the Yb^{3+}-doped NCS glass has stronger crystallization trend. The crystalline and micro-crystal phase of the Nd^{3+}- and Yb^{3+}-doped NCS glass-ceramics are 84.35 ± 5 vol% of $Na_6Ca_3Si_6O_{18}$ and 87.03 ± 5 vol% of $Na_4Ca_4Si_6O_{18}$, respectively.

Two kinds of micro-crystal phases in the Nd^{3+}-and Yb^{3+}-doped NCS glass-ceramics have same basic structural units composed of 6-membered rings formed by 6 [SiO_4] groups but the micro-crystals in the Yb^{3+}-doped NCS glass-ceramics have a composition ratio more similar to its parent glass.

The transmittances of the Yb^{3+}-doped NCS glass-ceramics from 400 nm to 1100 nm is higher than that of Nd^{3+}-doped NCS glass-ceramics for 3 mm sample. The absorptions of Nd^{3+}-doped NCS glass-ceramics appear at about 530 nm, 580 nm, 750 nm, 820 nm and 880 nm, while the absorption of Yb^{3+}-doped NCS glass-ceramics appears at about 975 nm.

The Nd^{3+}- and Yb^{3+}-doped NCS glass-ceramics show strong fluorescence emissions at 1060 nm and 975 nm, respectively. The results indicate that rare earth ions-doped highly crystalline transparent glass-ceramics have the potential for use as laser medium.

Acknowledgments

The research has been partially supported by the National Natural Science Foundation of China (No. 51172286).

References

[1] K. Ueno, K. Hattori, C. Idaa, S. Iwaki, S. Kabuki, H. Kuboa, S. Kurosawa, K. Miuchi, T. Nagayoshi, H. Nishimura, R. Oritoc, A. Takada, T. Tanimori, Performance of the gamma-ray camera based on GSO(Ce) scintillator array and PSPMT with the ASIC readout system, Nuclear Instruments and Methods A 591 (2008) 268–271.

[2] M. Kobayashi, S. Aogaki, F. Takeutchi, Y. Tamagawa, Y. Usuki, Performance of thin long scintillator strips of GSO:Ce, LGSO:Ce and LuAG:Pr for low energy γ-rays, Nuclear Instruments and Methods A 693 (2012) 226–235.

[3] S. Kurosawa, M. Sugiyama, T. Yanagida, Y. Yokota, A. Yoshikawa, Temperature dependence of the scintillation properties of Ce:GSO and Ce:GSOZ, Nuclear Instruments and Methods A 690 (2012) 53–57.

[4] B. Baiboussinov, C. Braggio, A. Cardini, G. Carugno, F. Congiu, S. Gain, G. Galeazzi, A. Lai, A. Lehman, P. Mocci, A. Mura, F. Quochi, M. Saba, B. Saitta, G. Sartori, An active electron polarized scintillating GSO target for neutrino physics, Nuclear Instruments and Methods A 694 (2012) 335–340.

[5] F. Ciocia, A. Braem, E. Chesi, R. De Leo, C. Joram, L. Lagamba, E. Nappi, J. Seguinot, I. Vilardi, P. Weilhammer, GEANT4 studies on the propagation and detection of scintillation light in long thin YAP crystals, Nuclear Instruments and Methods A 600 (2009) 506–512.

[6] D.H. Cao, G.J. Zhao, J.Y. Chen, Q. Dong, J. Zhu, H.G. Li, Growth and spectroscopic properties of RE, Mn:YAP (RE=Yb and Ce) photorefractive crystals, Journal of Luminescence 129 (10) (2009) 1169–1173.

[7] J. Liu, Y.G Wang, Z.S Qu, X.W Fan, 2 μm passive Q-switched mode-locked Tm^{3+}:YAP laser with single-walled carbon nanotube absorber, Optics and Laser Technology, 44, 960–962.

[8] M. Asadian, S.H. Seyedein, M.R. Aboutalebi, A. Maroosi, Optimization of the parameters affecting the shape and position of crystal–melt interface in YAG single crystal growth, Journal of Crystal Growth 311 (2) (2009) 342–348.

[9] M.F. Zhang, H.A.X. Guo, J.C. Han, H.L. Zhang, C.H. Xu, Distribution of Neodymium and properties of Nd:YAG crystal by horizontal directional solidification, Journal of Crystal Growth 340 (1) (2012) 130–134.

[10] J. Li, F. Chen, W.B. Liu, W.X. Zhang, L. Wang, X.W. Ba, Y.J. Zhu, Y. B. Pan, J.K. Guo, Co-precipitation synthesis route to yttrium aluminum garnet (YAG) transparent ceramics, Journal of the European Ceramic Society 32 (11) (2012) 2971–2979.

[11] J. Zhou, W.X. Zhang, T.D. Huang, L. Wang, J. Li, W.B. Liu, B.X. Jiang, Y.B. Pan, J.K. Guo, Optical properties of Er,Yb co-doped YAG transparent ceramics, Ceramics International 37 (2) (2011) 513–519.

[12] M. Asadian, N. Mirzaei, H. Saeedi, M. Najafi, I. Mashayekhi Asl, Improvement of Nd:GGG crystal growth process under dynamic atmosphere composition, Solid State Science 14 (2) (2012) 262–268.

[13] R. Soulard, B. Xu, J.L. Doualan, P. Camy, R. Moncorgé, Ground- and excited-state absorption and emission spectroscopy of Nd:GGG, Journal of Luminescence 132 (10) (2012) 2521–2524.

[14] E. Kubota, M. Shimokozono, Y. Katoh, LPE growth of yttrium–lutetium, indium–gallium garnet films for optical waveguide formation on a GGG substrate, Journal of Crystal Growth 191 (3) (1998) 501–511.

[15] E. Strassburger, Ballistic testing of transparent armour ceramics, Journal of the European Ceramic Society 29 (2009) 267–273.

[16] R. Klement, S. Rolc, R. Mikulikova, J. Krestan, Transparent armour materials, Journal of the European Ceramic Society 28 (2008) 1091–1095.

[17] A. Lu, Highly crystalline transparent glass ceramics: a challenging important research direction, Comments on Inorganic Chemistry 32 (2011) 277–288.

[18] V.M. Fokin, O.V. Potapov, E.D. Zanotto, F.M. Spiandorello, V. L. Ugolkov, B.Z. Pevzner, Mutant crystals in $Na_2O \cdot 2CaO \cdot 3SiO_2$ glasses, Journal of Non-Crystalline Solids 331 (2003) 240–253.

[19] V.M. Fokin, E.D. Zanotto, Continuous compositional changes of crystal and liquid during crystallization of a sodium calcium silicate glass, Journal of Non-Crystalline Solids 353 (24-25) (2007) 2459–2468.

[20] T. Berthier, V.M. Fokin, E.D. Zanotto, New large grain,highly crystalline, transparent glass-ceramic, Journal of Non-Crystalline Solids 354 (2008) 1721–1730.

[21] S.M. Wang, F.H. Kuang, Q.Z. Yan, Q.C. Zhang, C.C. Ge, Crystallization behavior of a new transparent glass-ceramics, Advanced Materials Research 105-106 (2010) 597-579.

[22] J. Li, Y.Z. Mei, C. Gao, F. Ren, A.X. Lu, Variation of luminescence properties of Na_2O–CaO–SiO_2: Nd^{3+} glass with crystallinity, Journal of Non-Crystalline Solids 357 (2011) 1736–1740.

[23] J. Li, Y.Z. Mei, Z.W. Luo, A.X. Lu, Preparation of transparent glass-ceramics with high crystallinity, Chinese Journal of Nonferrous Metals 21 (6) (2011) 1450–1456.

[24] P. Chimalawong, J. Kaewkhao, T. Kittiauchawal, C. Kedkaew, P. Limsuwan, Optical Properties of the SiO_2–Na_2O–CaO–Nd_2O_3 glasses, American Journal of Applied Sciences 7 (4) (2010) 584–589.

[25] Y.Z. Mei, X.J. Chen, K.Q. Wang, X.F. Liu, Z.W. Luo, A.X. Lu, Preparation and microstructure of Na_2O–CaO–SiO_2 transparent glass-ceramics, Chinese Journal of Nonferrous Metals 22 (7) (2012) 1991–1997.

[26] D.J. Yao, Zh.Y. Wang, P.R. Sundararajan, Time dependent crystal–smectic transformation in perylene-containing polyimides, Polymer 46 (2005) 4390–4396.

[27] Y. Tian, J.J. Zhang, X.F. Jing, S.Q. Xu, Optical absorption and near infrared emissions of Nd^{3+}doped fluorophosphate glass, Spectrochimica Acta Part A 98 (2012) 355–358.